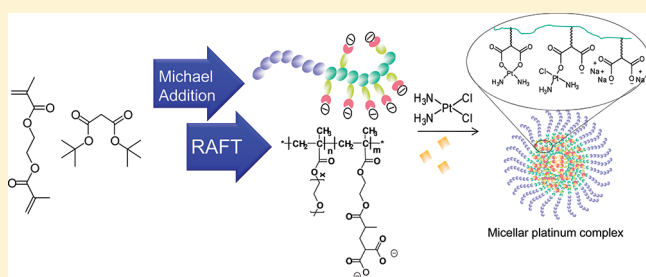


Polymeric Micelles with Pendant Dicarboxylato Chelating Ligands Prepared via a Michael Addition for *cis*-Platinum Drug DeliveryVien T. Huynh,<sup>†</sup> Paul de Souza,<sup>‡,§</sup> and Martina H. Stenzel<sup>†,\*</sup><sup>†</sup>Centre of Advanced Macromolecular Design (CAMD), The University of New South Wales, Sydney NSW 2052, Australia<sup>‡</sup>St. George Hospital Clinical School, The University of New South Wales, Sydney NSW 2052, Australia<sup>§</sup>Molecular Medicine Research Group, University of Western Sydney School of Medicine, Campbelltown, NSW, Australia

S Supporting Information

**ABSTRACT:** A new monomer with a neighboring carboxylate functional group was prepared via carbon Michael addition between ethylene glycol dimethacrylate and malonate. The monomer, 1,1-di-*tert*-butyl 3-(2-(methacryloyloxy)ethyl) butane-1,1,3-tricarboxylate (MAETC), was polymerized in a controlled manner using RAFT polymerization. After deprotection and the conjugation of platinum drugs, a macromolecular Pt complex was created, which was found to be insoluble in water. <sup>195</sup>Pt NMR revealed that the desired complex has been formed next to a minor fraction of other Pt complexes. Block copolymers were prepared using poly[oligo(ethylene glycol) methyl ether methacrylate] (POEGMEMA) as macroRAFT agent for chain extension with the synthesized monomer to yield three different block copolymers with varying PMAETC block lengths. Subsequent conjugation to platinum resulted in amphiphilic block copolymers, which can ultimately generate micelles. The length of the core block had significant contribution to the micelle sizes with the micelle size increasing with an increase of the hydrophobic block length. The polymers prior to platinum conjugation were found to be nontoxic when in contact with A549, a lung cancer cell line. After conjugation with the platinum drug, the micelle with the shortest PMAETC block length was found to have the highest toxicity, which may be due to the fastest cisplatin release when compared to the longer PMAETC block lengths.



## ■ INTRODUCTION

Platinum drugs are one of the most efficient drugs currently utilized to suppress the growth of a number of solid tumors including ovarian, bladder, testicular, head and neck, small-cell, and non small-cell lung cancers.<sup>1–3</sup> The activity of cisplatin [*cis*-dichlorodiamine platinum(II); CDDP], the parent of all the platinum drugs, and its second-generation analogues (i.e., oxaliplatin and carboplatin) have been well studied, and the results are summarized in the literature over the years.<sup>2,4–7</sup> However, their clinical toxicity and the development of drug resistance can cause major problems.<sup>2,8,9</sup> Cisplatin undergoes a range of nonselective binding events with a vast number of biomolecules including phospholipids and proteins in the body that reduce the activity of the drug on its way to the tumor. Despite adequate serum concentrations achieved from intravenous infusions, only a small proportion finds its way to the tumor to ultimately induce apoptosis by binding to DNA.<sup>10,11</sup> Moreover, the drug is distributed throughout the whole body upon administration and this produces dose-limiting nephro- and hepatotoxicities. Hence, better targeting of the drug to the DNA of cancerous cells would be highly advantageous, at least theoretically.

One of the most promising strategies to enhance targeting is to employ polymeric nanocarriers to achieve passive targeting via the enhanced permeation retention effect (EPR).<sup>12–14</sup> Nanoparticles

enable protection of cisplatin from undesirable binding events during drug distribution in the body, while facilitating the transport of the drug across the cell membrane via endocytosis at the site of action. Polymeric micelles, self-assembled block copolymers with a core–shell structure, are well-known as potential vehicles to target drugs, proteins, genes, and imaging agents to tumors.<sup>12</sup>

Platinum drugs consist typically of two permanently bound ligands, usually amines, and two labile leaving ligands, which are based on chlorides or carboxylate functional groups (Figure 1). Earlier research efforts in creating carrier-bound platinum complexes were aimed at the development of conjugates in which the two amine ligands were donated by the polymer either as main chain components or as side chain moieties. However, if the drug is tightly bound to the polymer, release is only possible via degradation of the polymer, and therefore, a macromolecular platinum drug, and not a drug carrier, has been created.<sup>15</sup> A different drug binding strategy involves the coordination via carboxylato ligands, thus permitting drug release via hydrolytically cleaved carboxyl leaving groups.<sup>16</sup> A range of polymers with inherent ligating groups such as poly(aspartic acid),<sup>17,18</sup> poly(glutamic acid),<sup>19</sup>

Received: July 19, 2011

Revised: September 2, 2011

Published: September 22, 2011

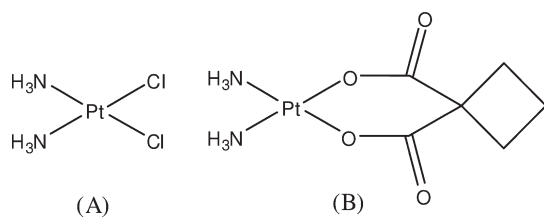


**Figure 1.** Cisplatin (A) and its second generation analogue carboplatin (B).

and poly(methacrylic acid)<sup>20</sup> have been employed to generate platinum–polymer complexes. The common feature of these polymers is that two ligands coordinate to platinum in nonspecific geometry, thus allowing cross-linking of polymer chains to take place.

More recent developments in platinum drug carrier design has shifted from monodentate carboxylato ligands to well-defined bidentate carboxylato ligands with usually 1,1- or 1,2-geometry resulting in the formation of chelate rings after coordination with platinum. The formation of 6–8 member rings with platinum promotes stability of the complex in solution resulting in structurally better defined platinum complexes. Polymers with bidentate ligands should therefore be more likely to result in soluble polymers with cross-linking being absent. Furthermore, this configuration of platinum complex is similar to carboplatin (Figure 1B), which shows reduced nephrotoxicity, is less toxic to the gastrointestinal tract, and is less neurotoxic compared to cisplatin (Figure 1A).<sup>2</sup> Although the adducts between carboplatin and DNA are exactly the same as those formed by cisplatin, 20–40 fold higher concentration of carboplatin are required, and the rate of binding to DNA is around 10-fold slower.<sup>21</sup> The design of AP5346, polymeric drug delivery system for platinum drugs, was inspired by this type. In this elegant approach, a statistical copolymer with 1,2-carboxylato ligands were created, although the subsequent Pt complex formation did not involve the form carboplatin derivatives but N,O-chelates were formed involving amide functionalities from the polymer side chain.<sup>22</sup> In our previous study, attempts to generate O,O'-chelates using 1,2-dicarboxylate ligand, which were clicked via thiol–ene chemistry to the backbone, led to the probable involvement of the thioether in the complex formation.<sup>23</sup>

So far, however, there has been little investigation on well-defined polymer architectures such as block copolymers with controlled molecular weight and bidentate ligands.

Two different approaches can be used for the synthesis of the requisite carrier polymer: polymerization of a dicarboxylato-containing monomer or postfunctionalization of preformed polymers using dicarboxylato moieties. In the previous study, a full investigation of postfunctionalized polymers with dicarboxylato groups and subsequent conjugation to platinum drugs were carried out. However, postfunctionalization leads to introduction of linkers that can potentially bind to platinum.<sup>23</sup> In contrast, the direct polymerization of a dicarboxylato-containing monomer could offer several advantages such as resulting in a fully functionalized polymer and fewer side-reactions.

The aim of this work was the preparation of monomers with bidentate carboxylato groups with the prerequisite to have any groups absent, which can potentially form complexes with Pt (Figure 2). To ensure the formation of carboplatin derivatives, malonates were conjugated to the polymers via the formation of C–C bonds and therefore any nitrogen and sulfur ligands were absent. The base-catalyzed Michael addition of a nucleophile

such as an enolate anion (Michael donor) to an activated  $\alpha,\beta$ -unsaturated carbonyl-containing compound (Michael acceptor) were chosen as a suitable avenue to create monomers with bidentate carboxylate ligands while other strongly ligating groups are absent.<sup>24</sup> RAFT polymerization was subsequently employed to synthesize block copolymers carrying bidentate carboxylato ligands with different varying block lengths. Platination can generate six-membered ring structures, which promotes the stability of the complex in the solution<sup>16,25</sup> while different block copolymers may produce a variety of micelle sizes (Figure 2).<sup>26</sup>

## EXPERIMENTAL PART

**Materials.** Unless otherwise specified, all chemicals were reagent grade and were used as received: di-*tert*-butyl malonate (Aldrich, 98%), ethylene glycol dimethacrylate (EGDMA, Aldrich, 98%), potassium carbonate (Univar, anhydrous), 18-crown-6 (Sigma-Aldrich, 99%), tetrahydrofuran (THF, anhydrous, 98%, Aldrich), diethyl ether (Et<sub>2</sub>O anhydrous, Ajax Finechem, 99%), petroleum ether (BR 40–60 °C; Ajax Finechem, 90%), ethyl acetate (EtOAc, Ajax Finechemicals, 99.5%), *N,N*-dimethylacetamide (DMAc; Aldrich, HPLC grade), magnesium sulfate (Ajax Finechem, 70%), toluene (Aldrich; purum), 1,4-dioxane (Sigma-Aldrich, 99%), chloroform-*d* (CDCl<sub>3</sub>; Cambridge Isotope Laboratories), cis-Dichlorodiaminoplatinum(II) (CDDP; Sigma-Aldrich; 99.9%), *o*-phenylenediamine (*o*-PDA; Hopkin and Williams).

2,2-Azobis(isobutyronitrile) (AIBN; Fluka, 98%) was purified by recrystallization from methanol. Oligo(ethylene glycol) methyl ether methacrylate (OEGMEMA; MW = 300 g mol<sup>-1</sup>; Aldrich) was deionized by passing through a column of basic aluminum oxide.

The RAFT agent (4-cyanopentanoic acid)-4-dithiobenzoate (CPADB) was synthesized according to literature<sup>27,28</sup> and recrystallized from toluene. Deionized (DI) water produced by a Mili-Q water purification system has a resistivity of 17.9 mΩ/cm.

**Analyses.** *Size Exclusion Chromatography (SEC).* SEC was implemented using a Shimadzu modular system comprising a DGU-12A degasser, a LC-10AT pump, a SIL-10AD automatic injector, a CTO-10A column oven, a RID-10A refractive index detector, and a SPD-10A Shimadzu UV/vis detector. A 50 × 7.8 mm guard column and four 300 × 7.8 mm linear columns (500, 10<sup>3</sup>, 10<sup>4</sup>, and 10<sup>5</sup> Å pore size, 5 μm particle size) were used for the analyses. *N,N*-dimethylacetamide (DMAc) (HPLC grade, 0.05% w/v of 2,6-dibutyl-4-methylphenol (BHT), 0.03% w/v of LiBr) with a flow rate of 1 mL min<sup>-1</sup> and a constant temperature of 50 °C was used as the mobile phase with an injection volume of 50 μL. The samples were filtered through 0.45 μm filters. The unit was calibrated using commercially available linear polystyrene standards (0.5–1000 kDa, Polymer Laboratories). Chromatograms were processed using Cirrus 2.0 software (Polymer Laboratories).

*Nuclear Magnetic Resonance (NMR) Spectroscopy.* <sup>1</sup>H and <sup>13</sup>C NMR spectra were recorded using a Bruker ACF300 (300 MHz) spectrometer, with (CD<sub>3</sub>)<sub>2</sub>SO, CD<sub>3</sub>OD, or CDCl<sub>3</sub> used as solvents. All chemical shifts are stated in ppm (δ) relative to tetramethylsilane (δ = 0 ppm), referenced to the chemical shifts of residual solvent resonances (<sup>1</sup>H and <sup>13</sup>C). The number of scan was 16 as default for all polymer samples. For <sup>195</sup>Pt NMR measurement, <sup>195</sup>Pt resonances were externally referenced to Na<sub>2</sub>PtCl<sub>6</sub> at 0 ppm. Spectra were obtained using a broadband observe 5 mm probe with *z*-axis gradient capability. The Bruker pulse program zgpgmultiscan was modified to execute a very short delay time (set at *d*<sub>1</sub> = 2 ms) followed by a hard 90° pulse. The experiment was run in increments of 20 000 scans (ns = 20 000) over a 130 kHz sweep width (9 ms acquisition time). A loop counter parameter 13 = 100 was incorporated such that the initial iteration of 20 000 scans was repeated 90 times to give an accumulated number of 2 000 000 scans (FIDs from each iteration were automatically combined and Fourier transformed to produce the frequency domain spectrum).

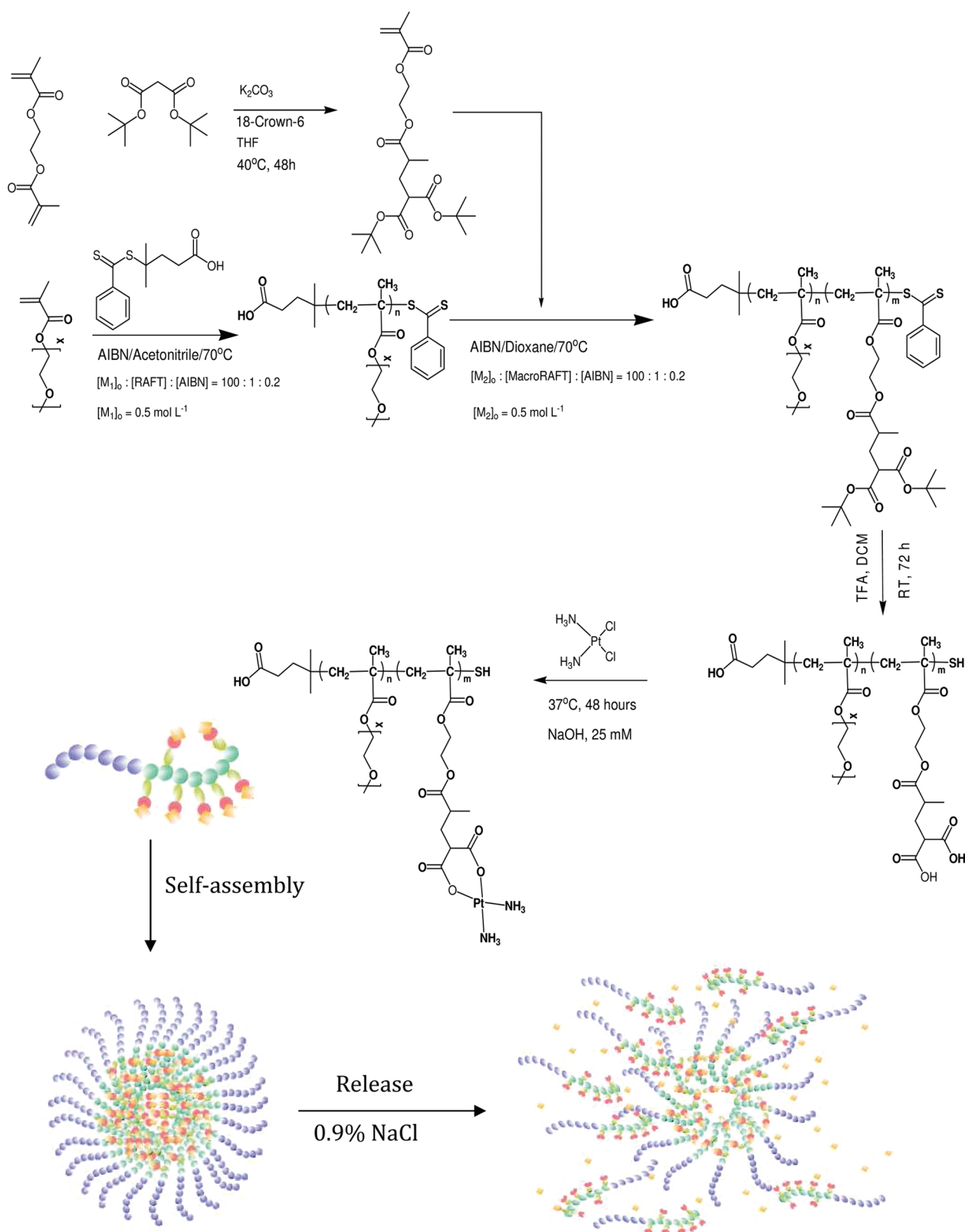


**Figure 2.** Monomer synthesis via Michael addition and subsequent synthesis of block copolymers via RAFT polymerization, followed by the conjugation of Pt drugs and the formation of micelles, and release of platinum from polymeric platinum micelles.

*Dynamic Light Scattering (DLS).* The average hydrodynamic diameters  $D_h$  and size distributions of the prepared micelle solution in an aqueous solution (1 mg mL<sup>-1</sup>) were measured using a Malvern

ZetasizerNano ZS instrument equipped with a 4 mV He–Ne laser operating at  $\lambda = 632$  nm, an avalanche photodiode detector with high quantum efficiency, and an ALV/LSE-5003 multiple- $\tau$  digital



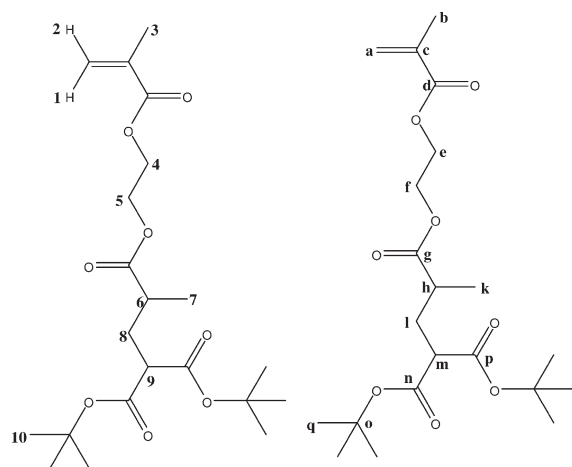


**Figure 3.** Monomer with  $^1\text{H}$  NMR (left) and  $^{13}\text{C}$  NMR (right) label.

correlator electronics system. The samples were filtered to remove dust using a microfilter ( $0.45\ \mu\text{m}$ ) prior to measurement.

**Transmission Electron Microscopy (TEM).** Analyses were performed using a JEOL 1400 TEM with a beam voltage of 100 kV and a Gatan CCD for acquisition of digital images. Samples were prepared by placing a droplet of a  $1\ \text{mg mL}^{-1}$  polymer solution on a formamide and graphite coated copper grid and draining the excess using filter paper after 60 s. To negatively stain the samples a droplet of 2% (w/v) phosphotungstic acid solution was placed on the copper grid for 30 s before being drained with filter paper.

**Thermo Gravimetric Analysis (TGA).** Thermal decomposition properties of polymers were recorded using a Perkin-Elmer thermogravimetric analyzer (Pyris 1 TGA). Analyses were conducted over a temperature range of 30–700 °C with a programmed temperature increment of 20 K per min.

**Inductively Coupled Plasma-Mass Spectrometer (ICP-MS).** The Perkin-Elmer ELAN 6000 inductively coupled plasma-mass spectrometer (Perkin-Elmer, Norwalk, CT) was used for quantitative determinations of platinum. All experiments were carried out at an incident ratio frequency power of 1200 W. The plasma argon gas flow of  $12\ \text{L min}^{-1}$  with an auxiliary argon flow of  $0.8\ \text{L min}^{-1}$  was used in all cases. The nebulizer gas flow was adjusted to maximize ion intensity at  $0.93\ \text{L min}^{-1}$  as indicated by the mass flow controller. The element/mass detected was  $^{195}\text{Pt}$  and the internal standard used was  $^{193}\text{Ir}$ . Replicate time was set to 900 ms and the dwell time to 300 ms. Peak hopping was the scanning mode employed and the number of sweeps/readings was set to 3. Ten replicates were measured at a normal resolution. The samples were treated with aqua regia solution at 90 °C for 2 h to digest platinum.

**Synthesis.** *Synthesis of 1,1-di-tert-Butyl 3-(2-(Methacryloyloxy)ethyl) Butane-1,1,3-tricarboxylate (MAETC).* In a typical experiment, ethylene glycol dimethacrylate (EGDMA, 2.657 g, 13.4 mmol, 3 equiv), potassium carbonate (0.679 g, 4.9 mmol, 1.1 equiv), and 18-crown-6 (0.039 g, 0.15 mmol, 0.033 equiv) as a catalyst were added to 0.7 mL of anhydrous THF and the mixture was cooled to 0 °C in an ice bath before degassing under nitrogen for 30 min. Di-tert-butyl malonate (0.966 g, 4.5 mmol, 1 equiv) was added dropwise with vigorous stirring. The slurry suspension was stirred for 30 min while maintaining the temperature at 0 °C then stirred for a further 48 h at 40 °C. The color changed from no color to yellowish. The deionized (DI) water (15 mL) was added into the slurry before being washed three times with diethyl ether ( $3 \times 30\ \text{mL}$ ) using a separation funnel. The diethyl ether phases were combined and evaporated using the rotary evaporator. The residual oily liquid was purified by silica gel column chromatography using petroleum spirit/ethyl acetate mixture as gradient eluent with the ratio from 20:1 to 8:1, v/v. The collected fractions were examined by TLC (stained by

permanganate solution). The product ( $R_f = 0.3$ ) was obtained as an oily yellowish liquid (61% in yield) and characterized by  $^1\text{H}$  and  $^{13}\text{C}$  NMR spectroscopy (Figure 3) and ESI–MS. The liquid solidified into crystals when left in a freezer overnight.  $^1\text{H}$  NMR (300.17 MHz,  $\text{CDCl}_3$ , 25 °C):  $\delta$  (ppm) = 6.12 (s, 1H,  $\text{H}_1$ ), 5.58 (s, 1H,  $\text{H}_2$ ); 4.34 (t, 4H,  $\text{H}_4$  and  $\text{H}_5$ ,  $J = 1.08\ \text{Hz}$ ); 3.2–3.25 (dd, 1H,  $\text{H}_6$ ,  $J = 6.45\ \text{Hz}$ ,  $J = 8.91\ \text{Hz}$ ); 2.45–2.57 (qq, 1H,  $\text{H}_6$ ,  $J = 6.99\ \text{Hz}$ ); 2.15 (dd, 1H,  $\text{H}_8$ ,  $J = 6.54\ \text{Hz}$ ); 1.9 (dd, 4H,  $\text{H}_8$  and  $\text{H}_3$ ,  $J = 6.12\ \text{Hz}$ ); 1.43 (s, 18H,  $\text{H}_{10}$ ); 1.18 (d, 3H,  $\text{H}_7$ ,  $J = 7.02\ \text{Hz}$ ).

$^{13}\text{C}$  NMR (75.48 MHz,  $\text{CDCl}_3$ , 25 °C):  $\delta$  (ppm) = 175.37 ( $\text{C}_g$ ), 168.41 ( $\text{C}_n$ ), 168.21 ( $\text{C}_p$ ), 166.99 ( $\text{C}_d$ ), 135.79 ( $\text{C}_c$ ), 126.01 ( $\text{C}_a$ ), 81.50 ( $\text{C}_o$ ), 62.33 ( $\text{C}_e$ ), 61.99 ( $\text{C}_f$ ), 51.64 ( $\text{C}_m$ ), 37.08 ( $\text{C}_h$ ), 31.96 ( $\text{C}_l$ ), 27.79 ( $\text{C}_q$ ), 18.18 ( $\text{C}_b$ ), 17.30 ( $\text{C}_k$ ). See ESI-Figure S1 in Supporting Information for full spectra.

ESI–MS: calcd for  $\text{C}_{21}\text{H}_{34}\text{O}_8$ , 414.23; found 437.1 ( $\text{Na}^+$ ).

**Polymer Synthesis.** *RAFT Polymerization of MAETC Using CPADB RAFT Agent.* MAETC ( $0.866\ \text{g}$ ,  $2.09 \times 10^{-3}\ \text{mol}$ ), CPADB ( $5.84 \times 10^{-3}\ \text{g}$ ,  $2.09 \times 10^{-5}\ \text{mol}$ ) as RAFT agent, and AIBN ( $0.69 \times 10^{-3}\ \text{g}$ ,  $4.18 \times 10^{-6}\ \text{mol}$ ) as initiator were dissolved in toluene (1.73 mL) in a 10 mL vial to give  $[\text{MAETC}]:[\text{CPADB}]:[\text{AIBN}] = 100:1:0.2$  and  $[\text{MAETC}] = 1.21\ \text{mol L}^{-1}$ . The solution was divided into seven small vials, which were deoxygenated using nitrogen purging. The small vials were placed into a constant temperature oil bath at 70 °C. Each vial was collected at regular time intervals and plunged immediately into an ice bath to cease the polymerization. The final solution was precipitated into chilled hexane, followed by centrifuging to give a pink waxy polymer. After a polymerization time of 7 h,  $^1\text{H}$  NMR reveals a monomer conversion of 70% ( $M_{n,\text{theo}} = 29,294\ \text{g mol}^{-1}$ ,  $M_{n,\text{SEC}} = 19,300\ \text{g mol}^{-1}$ , PDI = 1.12).  $^1\text{H}$  NMR (300.17 MHz, acetone- $d_6$ , 25 °C):  $\delta$  (ppm) = 8.0–7.4 (aromatic ring of CPADB), 4.5–4.0 (4nH,  $\text{OCH}_2\text{CH}_2\text{O}$ ), 3.4–3.2 (nH, *tert*-Bu– $\text{OOCCH}(\text{CH}_2)\text{COO}$ –*tert*-Bu), 2.7–2.4 (nH,  $(\text{C}=\text{O})\text{CH}(\text{CH}_3)\text{--CH}_2$ ), 2.3–2.1 (nH,  $(\text{C}=\text{O})\text{CH}(\text{CH}_3)\text{--CH}_2\text{CH}$ ), 2.1–1.8 (nH,  $(\text{C}=\text{O})\text{CH}(\text{CH}_3)\text{--CH}_2\text{CH}$ ), 1.6–1.4 (18nH,  $(\text{C}=\text{O})\text{--OCH}(\text{CH}_3)_3$ ), 1.4–1.2 (3nH,  $\text{CH}_3$  of the main chain), 1.2–0.9 (2nH,  $\text{CH}_2$  of the main chain).  $n$  is the degree of polymerization ( $\text{DP}_n$ ) of PMAETC.

*Deprotection of the t-Bu Group from Block Copolymer of PMAETC and POEGMEMA.* In a typical experiment, POEGMEMA-*block*-PMAETC (10 mg,  $4.57 \times 10^{-7}\ \text{mol}$ ) and trifluoroacetic acid ( $4 \times 10^{-5}\ \text{mg}$ ,  $4.57 \times 10^{-6}\ \text{mol}$ ) were added to dichloromethane (0.8 mL) in the Schlenk tube. The tube was sealed and reacted at room temperature with stirring for 72 h. The final reaction mixture was then dialyzed in a 1000 molecular weight cutoff (MWCO) dialysis membrane against acetone–water (1:1) as solvent. The solvent was replaced in regular intervals of 3 h during the dialysis course, followed by dialysis against pure water. Subsequently, the remaining solution inside the bag was freeze-dried to yield a white waxy polymer. The deprotected copolymers were characterized by GPC and  $^1\text{H}$  NMR.  $^1\text{H}$  NMR (300.17 MHz, acetone- $d_6$ , 25 °C):  $\delta$  (ppm) = 4.5–4.0 (4nH,  $\text{OCH}_2\text{CH}_2\text{O}$ ), 3.6–3.4 (nH,  $\text{HOOCCHCH}_2\text{COOH}$ ), 2.7–2.4 (nH,  $\text{OOCCHCH}_2\text{CH}_2$ ), 2.3–2.1 (nH,  $\text{OOCCHCH}_2\text{CH}_2\text{CH}$ ), 2.1–1.8 (nH,  $\text{OOCCHCH}_2\text{CH}_2\text{CH}$ ), 1.4–1.2 (3nH,  $\text{CH}_3$  of the main chain), 1.2–0.9 (2nH,  $\text{CH}_2$  of the main chain).  $n$  is the degree of polymerization ( $\text{DP}_n$ ) of PMAETC.

*RAFT Polymerization of OEGMEMA Using CPADB RAFT Agent.* OEGMEMA (7.0 g,  $2.3 \times 10^{-2}\ \text{mol}$ ), CPADB (0.065 g,  $2.3 \times 10^{-4}\ \text{mol}$ ) as RAFT agent, and AIBN (0.0077 g,  $4.67 \times 10^{-5}\ \text{mol}$ ) as initiator were dissolved in toluene (46.62 mL) in a 100 mL round-bottom flask to give  $[\text{OEGMEMA}]:[\text{CPADB}]:[\text{AIBN}] = 100:5:0.2$  and  $[\text{OEGMEMA}] = 0.5\ \text{mol L}^{-1}$ . The solution was divided into aliquots, sealed by rubber septum and thoroughly deoxygenated using nitrogen purging for 45 min before placed in a constant temperature oil bath at 70 °C. Samples were taken out at regular time intervals and analyzed via  $^1\text{H}$  NMR to determine the conversion, followed by precipitating in petroleum spirit. The final macroRAFT agent was characterized by GPC and  $^1\text{H}$  NMR.  $^1\text{H}$  NMR (300.17 MHz,  $\text{CDCl}_3$ , 25 °C):  $\delta$  (ppm) = 4.4–4.2 (2nH,  $\text{CH}_3\text{COOCH}_2\text{--CH}_2\text{O}$ ), 4.0–3.8 (11nH,  $\text{CH}_2$  of OEGMEMA monomer), 3.6–3.4 (3nH,  $\text{CH}_3$  of chain end of OEGMEMA), 1.4–1.2 (3nH,  $\text{CH}_3$  of the main chain),

1.2–0.9 ( $2nH$ ,  $CH_2$  of the main chain).  $n$  is the degree of polymerization ( $DP_n$ ) of POEGMEMA.

**Chain Extension of Poly(OEGMEMA) as MacroRAFT Agent with MAETC.** A batch of POEGMEMA (4 g) was synthesized using acetonitrile as a solvent to target a theoretical molecular weight of  $12\,000\text{ g mol}^{-1}$  by polymerizing OEGMEMA for 3 h using CPADB under identical conditions as those described previously ( $X_{NMR} = 50\%$ ,  $M_{n,theo} = 15,279\text{ g mol}^{-1}$ ,  $M_{n,SEC} = 11\,100\text{ g mol}^{-1}$ ,  $PDI = 1.06$ ). MAETC (0.1225 g,  $3.03 \times 10^{-4}\text{ mol}$ ), POEGMEMA ( $M_{n,theo} = 15,279\text{ g mol}^{-1}$ ,  $M_{n,SEC} = 11\,100\text{ g mol}^{-1}$ ,  $PDI = 1.06$ ,  $0.046\text{ g}$ ,  $3.03 \times 10^{-6}\text{ mol}$ ) as MacroRAFT agent, and AIBN ( $10^{-4}\text{ g}$ ,  $6.06 \times 10^{-7}\text{ mol}$ ) were dissolved in 0.6 mL of dioxane to result in  $[MAETC]:[POEGMEMA]:[AIBN] = 100:1:0.2$  and  $[MAETC] = 0.5\text{ mol L}^{-1}$ . The vial was capped with a rubber septum, paraffin film, and copper wire. Six vials of the solution were thoroughly deoxygenated using nitrogen purging for 45 min and then placed in a oil bath at  $70\text{ }^\circ\text{C}$ . Sample were taken every 1 h up to 6 h and quenched in an ice bath. The final copolymer was characterized by GPC and  $^1H$  NMR.  $^1H$  NMR (300.17 MHz,  $CDCl_3$ ,  $25\text{ }^\circ\text{C}$ ):  $\delta$  (ppm) = 4.3–4.0 ( $4mH$ ,  $OCH_2CH_2O$ ), 4.0–3.8 ( $2nH$ ,  $COOCH_2CH_2OCH_2CH_2O$ ), 3.8–3.5 ( $11nH$ ,  $COOCH_2CH_2OCH_2CH_2O$ ), 3.5–3.3 ( $3nH$ ,  $OCH_2CH_2OCH_2CH_2OCH_3$ ), 3.3–3.1 ( $mH$ , *tert*-Bu– $OOCCHCH_2COO$ –Bu-*tert*), 2.6–2.4 ( $mH$ ,  $OOCCHCH_3CH_2$ ), 2.3–2.0 ( $mH$ ,  $OOCCHCH_3CH_2CH(COO$ –Bu-*tert*) $_2$ ), 2.0–1.6 ( $mH$  +  $3mH$  +  $3nH$ ,  $OOCCHCH_3CH_2CH(COO$ –Bu-*tert*) $_2$ ,  $CH_3$  attached to the backbone of MAETC,  $CH_3$  attached to the backbone of OEGMEMA, respectively), 1.5–1.3 ( $18mH$ ,  $OOCCHCH_3CH_2CH(COO(CH_3)_3)_2$ ), 1.3–1.1 ( $3nH$ ,  $CH_3$  of the main chain), 1.1–0.7 ( $2nH$  +  $2mH$ ,  $CH_2$  of the main chain of OEGMEMA and  $CH_2$  of the main chain of MAETC, respectively).  $n$  and  $m$  are the degrees of polymerization ( $DP_n$ ) of POEGMEMA and PMAETC, respectively.

**Deprotection of Block Copolymers.** Deprotection of *tert*-butyl groups of block copolymers was carried out similar to the procedure mentioned above. The deprotected copolymer was characterized by  $^1H$  NMR, COSY–NMR, and HSQC–NMR.  $^1H$  NMR (300.17 MHz, acetone- $d_6$ ,  $25\text{ }^\circ\text{C}$ ):  $\delta$  (ppm) = 4.3–4.0 ( $4mH$ ,  $OCH_2CH_2O$ ), 4.0–3.8 ( $2nH$ ,  $COOCH_2CH_2OCH_2CH_2O$ ), 3.8–3.5 ( $11nH$ ,  $OCOCH_2CH_2OCH_2CH_2OCH_3$ ), 3.5–3.3 ( $3nH$ ,  $OCH_2CH_2OCH_2CH_2OCH_3$ ), 3.3–3.1 ( $mH$ , *tert*-Bu– $OOCCHCH_2COO$ –Bu-*tert*), 2.6–2.4 ( $mH$ ,  $OOCCHCH_3CH_2$ ), 2.3–2.0 ( $mH$ ,  $OOCCHCH_3CH_2CH(COO$ –Bu-*tert*) $_2$ ), 2.0–1.6 ( $mH$  +  $3mH$  +  $3nH$ ,  $OOCCHCH_3CH_2CH(COO$ –Bu-*tert*) $_2$ ,  $CH_3$  attached to the backbone of MAETC,  $CH_3$  attached to the backbone of OEGMEMA, respectively), 1.5–1.3 ( $18mH$ ,  $OOCCHCH_3CH_2CH(COO(CH_3)_3)_2$ ), 1.3–1.1 ( $3nH$ ,  $CH_3$  of the main chain), 1.1–0.7 ( $2nH$  +  $2mH$ ,  $CH_2$  of the main chain of POEGMEMA and  $CH_2$  of the main chain of PMAETC, respectively).  $n$  and  $m$  are the degrees of polymerization ( $DP_n$ ) of POEGMEMA and PMAETC, respectively.

**Polymer–Platinum Conjugates.** Conjugation of cisplatin to the polymer was described in previous works, but some modifications have been introduced here.<sup>29,30</sup> In a typical experiment, CDDP (10 mg) was suspended in 10 mL distilled water and mixed with silver nitrate ( $[AgNO_3]/[CDDP] = 1.955$ ) to form the aqueous complex. The solution was stirred in the dark at room temperature for 4 h. A white precipitate of silver chloride was observed indicative of the proceeding reaction. The mixture was then centrifuged at 9000 rpm for 20 min to remove the AgCl precipitates and the supernatant was purified by passing through a  $0.22\text{ }\mu\text{m}$  filter. Polymers with carboxyl functional groups (25 mg, dissolved in 2 mL of NaOH ( $1\text{ mg mL}^{-1}$ )) were added to above CDDP aqueous solution and left to react in a water bath at  $37\text{ }^\circ\text{C}$  for 12 h with gentle shaking to result in polymer–CDDP conjugates. The prepared conjugate was purified by Ultrafiltration using Sartorius Vivaspin 6 centrifugal filter devices with a molecular weight cut off of 3000 Da and then freeze-dried. The final product was a yellow powder.

**Release of Platinum Drug from Polymeric Platinum Conjugates.** Polymeric platinum conjugates (10 mg) was dissolved in

saline water 0.9% NaCl (pH 7.0) and dialyzed (cellulose tubing with molecular weight cut off approximately 3500 Da) against saline 0.9% solution (250 mL) at  $37\text{ }^\circ\text{C}$ . Aliquots of 1 mL were taken in regular time intervals from the dialysate over 168 h. The amount of released Pt was determined using inductively coupled plasma mass spectroscopy (ICP–MS). To a 10 mL centrifuge tube, 1 mL of the dialysate was diluted five times by aqua regia 2% ( $HCl:HNO_3 = 3:1$ ). The solution was then digested at  $60\text{ }^\circ\text{C}$  for 3 h before cooled down to room temperature. The concentration of Pt released from the conjugate was expressed as a ratio of the amount platinum in the releasing solution and that in the initial sample. The percentage of Pt released was calculated using

$$\% \text{ release} = \frac{V_{total}(t) \times C + Y}{Z}$$

where  $V_{total}(t)$  is the remaining volume in the releasing container at time  $t$  in mL;  $C$  is the concentration of platinum determined from ICP–MS in  $\mu\text{g mL}^{-1}$ ,  $Y$  is the amount of platinum that has already been collected in  $\mu\text{g}$ , and  $Z$  is the total amount of platinum at  $t = 0$  present in the dialysis bag in  $\mu\text{g}$

**Cytotoxicity Assay.** All micelle solutions of Pt–polymer conjugates were prepared using dialysis method. In a typical experiment, 10 mg of polymer (BP-E27/Pt) was fully dissolved in DMF, followed by adding dropwise 3 mL of DI water. Subsequent dialysis against DI water yield  $\sim 2.5\text{ mg mL}^{-1}$  micelle solution. The solutions were diluted with DI water to obtain the desired concentrations.

The Sulforhodamine B (SRB) assay established by the U.S. National Cancer Institute for rapid, sensitive, and inexpensive screening of antitumor drugs in microplates was employed to screen the cytotoxicity and antitumor activities of polymers and polymeric platinum drugs, respectively.<sup>31</sup> Human nonsmall lung cancer cells (NSCLC, A549) diluted in 100  $\mu\text{L}$  of RPMI-1640 medium (2 mM L-glutamine,  $1.5\text{ g L}^{-1}$  sodium bicarbonate, 10 mM HEPES,  $4.5\text{ g L}^{-1}$  glucose, 1 mM sodium pyruvate) were seeded into the wells with 2000 cells/well. The microtiter plates were left for 24 h at  $37\text{ }^\circ\text{C}$  and then exposed to various doses of polymers and micelles for 72 h. Cell cultures were fixed with TCA (10%, w/v) and incubated at  $4\text{ }^\circ\text{C}$  for 1 h. The wells were then washed five times with tap water to remove TCA, growth medium and low molecular weight metabolites. Plates were air-dried and then stored until use. TCA-fixed cells were stained for 30 min with 0.4% (w/v) SRB dissolved in 1% (v/v) acetic acid. At the end of the staining period, SRB was removed and cultures were quickly rinsed five times with 1% (v/v) acetic acid to remove unbound dye. Subsequently, the cultured plates were air-dried until no conspicuous moisture was visible before bound dye was shaken in 100  $\mu\text{L}$  of 10 mM Tris base for 5 min. The absorbance at 570 nm of each well was measured using microtiter plate reader Scanning spectrophotometer (Bio Tek's PowerWave HT Microplate Reader and KC4 Software). Each sample was replicated three times.

## RESULTS AND DISCUSSION

**Synthesis of Homopolymer and Conjugation to Platinum Drugs.** Focus of this project is the design of polymers with pendant bidendate carboxylate ligands, which can be utilized as macromolecular ligand. Since metals are inherently susceptible to undergo coordination complex formation with a range of functional groups, a pathway was chosen to generate structures with mainly C–C bonds leaving only ester groups as potentially interfering groups. Therefore, we opted for the efficient Michael Addition between malonates and vinyl functionalities to achieve this goal. The mechanism of this reaction, where every step is in equilibrium and thermodynamically dependent on the relative strengths of the base and the types of Michael donor, is well documented in the literature.<sup>32</sup> The acetoacetate is deprotonated

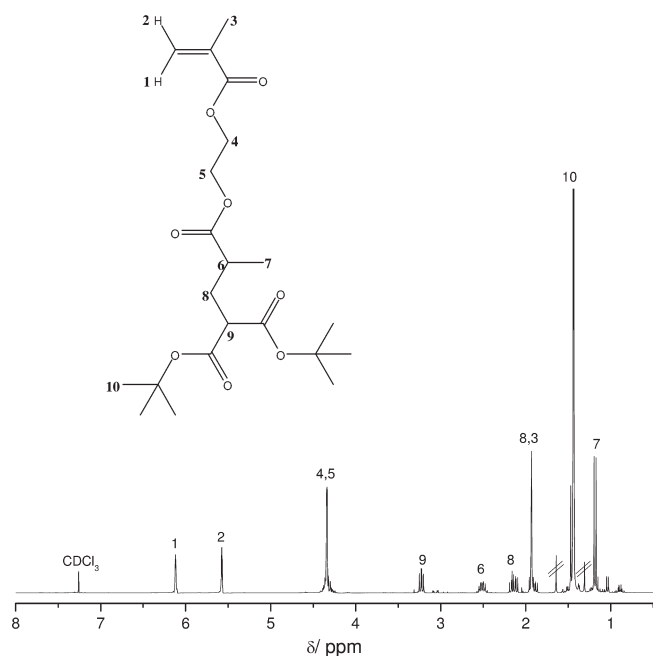


**Figure 4.**  $^1\text{H}$  NMR of the monomer 1,1-di-*tert*-butyl 3-(2-(methacryloyloxy)ethyl) butane-1,1,3-tricarboxylate (MAETC).

by strong base to form an enolate anion (Michael donor) in equilibrium. The enolate anion then reacts in a 1,4-conjugate addition to the olefin of the acrylate (Michael acceptor).<sup>32</sup> Many parameters (i.e., base strength,<sup>33</sup> solvents,<sup>34,35</sup> substrates<sup>36</sup>) been well studied over the years and have significant effects on the reaction rate.

A very simple and cheap way is the reaction of di-*tert*-butyl malonate with ethylene glycol dimethacrylate (EGDMA). Excess EGDMA leads to functionalization of only one methacrylate group while the remaining methacrylate group is available for the subsequent polymerization. The Michael addition between malonate and cross-linker to generate polymers via step-growth polymerization has been reported earlier as an efficient high yield process to polymers.<sup>32</sup> Here, this procedure was adopted for the reaction between di-*tert*-butyl malonate and EGDMA to generate a new monomer. Di-*tert*-butyl malonate was deprotonated in the presence of strongly alkaline condition prior to reaction with the double bond of EGDMA. Excess base (1.1 equiv compared to mole of the malonate) ensures the efficient deprotonation of the methylene group yielding the complete nucleophilic addition of all malonates. Interestingly, while the carbonate anion ( $\text{pK}_a = 8.5$ ) is not very alkaline in aqueous media, it is reactive enough in organic solvents to remove the proton from the active methylene of the malonate. To aid the low solubility of potassium carbonate in organic solvent, a phase transfer catalyst, 18-crown-6, was added. The crown ether plays an important role in this reaction as a result of its ability to solvate alkali metal in nonpolar or aprotic solvents such as THF.<sup>37,38</sup> The final yield of the monomer synthesis after purification was 61% and the monomer structure was confirmed by ESI-MS,  $^1\text{H}$  NMR,  $^{13}\text{C}$  NMR, DEPT-135, and DEPT-90. Visible changes in the  $^1\text{H}$  NMR spectra include a doublet of doublet at 3.25 ppm (Figure 4), which refers to the methine group between two carboxylates. It is also worth noting that the protons of methylene next to malonate have different chemical shifts (1.9 and 2.15 ppm, respectively). In addition to  $^1\text{H}$  NMR,  $^{13}\text{C}$  NMR, DEPT-135, and DEPT-90 confirmed the

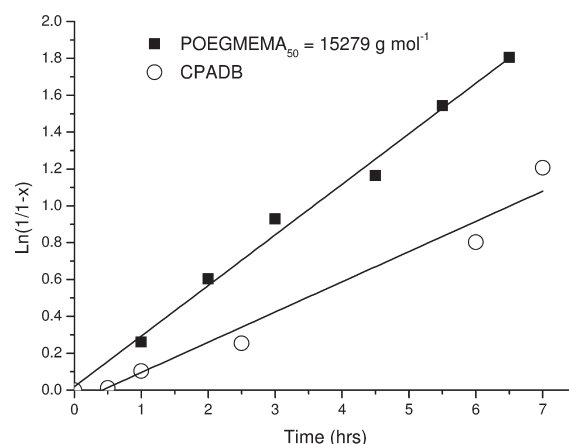


**Figure 5.** First order kinetic plot of the polymerization of MAETC at 70 °C in the presence of RAFT agent CPADB and macro RAFT agent POEGMEMA<sub>50</sub> ( $[\text{MAETC}] = 0.5 \text{ mol L}^{-1}$ ,  $[\text{RAFT}]$  or  $[\text{MacroRAFT}] = 0.5 \times 10^{-2} \text{ mol L}^{-1}$ ,  $[\text{AIBN}] = 0.1 \times 10^{-2} \text{ mol L}^{-1}$  in dioxane).

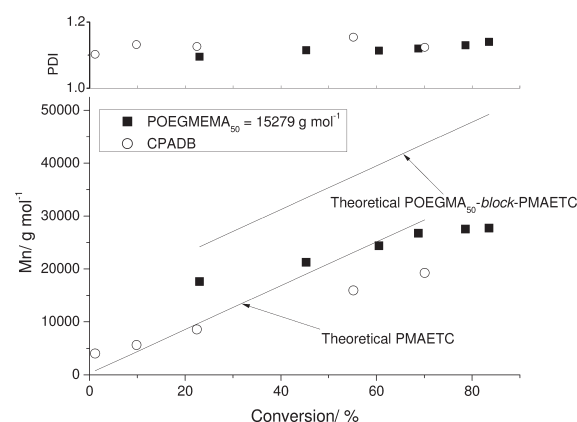


**Figure 6.** Number-average molecular weight  $M_n$  obtained by SEC and polydispersity index (PDI) against monomer conversion  $x$  for the polymerization of MAETC at 70 °C in the presence of RAFT agent CPADB and macro RAFT agent POEGMEMA<sub>50</sub> ( $[\text{MAETC}] = 0.5 \text{ mol L}^{-1}$ ,  $[\text{RAFT}] = 0.5 \times 10^{-2} \text{ mol L}^{-1}$ ,  $[\text{AIBN}] = 0.1 \times 10^{-2} \text{ mol L}^{-1}$  in dioxane).

structure as shown (ESI, Figure S1, Supporting Information). The molecular weight ESI-MS of the monomer was 437.1 ( $\text{Na}^+$ ), which is in agreement with the calculated molecular weight of 414.23 (437.23  $\text{Na}^+$ ).

Although the synthesis of block copolymers were the main aim of this work, the RAFT homopolymerization of this new monomer was investigated to evaluate the feasibility of this monomer to undergo a living process. In order to understand the polymerization behavior of this monomer, MAETC was polymerized at 70 °C using the  $[\text{MAETC}]:[\text{CPADB}]:[\text{AIBN}]$  ratio of 100:1:0.2 and a monomer concentration of  $1.2 \text{ mol L}^{-1}$  in toluene. The conversion of the monomer was calculated using  $^1\text{H}$  NMR spectroscopy comparing the intensity of vinyl proton peaks (6.12 and 5.58 ppm) to that of aliphatic proton peaks (1.1–1.3 ppm). As depicted in Figure 5, an inhibition period of about 30 min was observed before the polymerization proceeded with pseudo first order kinetics. This indicated that the radical concentration was constant during the course of polymerization and the conversion reached nearly 70% within 7 h. Interestingly, this inhibition period was only observed in the RAFT polymerization



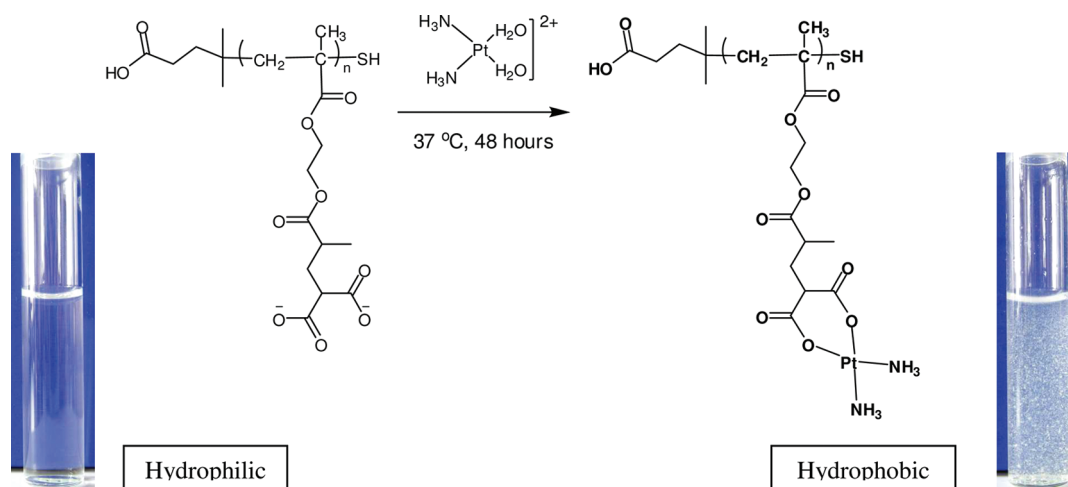


Figure 7. Formation of macromolecular Pt complexes confirmed by the change of solubility in water.

of MAETC in the presence of CPADB as RAFT agent, but not in the case of POEGMEMA (molecular weight of  $15300 \text{ g mol}^{-1}$ ). This is typical for the slow fragmentation of the initial of the initial RAFT agent since the stability of the leaving group is different to the methacrylate radical. In contrast, the leaving group of the macroRAFT agent is of similar stability since both, macroradical and leaving group, are methacrylate.<sup>39</sup>

The SEC chromatograms in ESI-Figure S2 (Supporting Information) confirm the shift of the molecular weights toward higher values with increasing reaction time. The measured and theoretical molecular weights and PDI in dependency on the monomer conversion are displayed in Figure 6. The SEC molecular weight increased almost linearly with conversion while the molecular weight distribution remain narrow ( $\text{PDI} < 1.13$ ).

PMAETC, which was prepared by polymerizing MAETC for 4 h using CPADB under identical conditions as those described previously, was isolated for further analysis. The final PMAETC homopolymer has a theoretical molecular weight of  $33\,000 \text{ g mol}^{-1}$  ( $\sim 79$  repeating units), SEC molecular weight of  $21,200 \text{ g mol}^{-1}$  and PDI of 1.09 (ESI, Figure S3, Supporting Information). The *tert*-butyl groups of PMAETC were removed by using concentrated trifluoroacetic acid (TFA) and dichloromethane as solvent at room temperature for 72 h. The subsequent purification was carried out by dialysis against a mixture of acetone and water followed by pure water. The polymer was freeze-dried before characterization by  $^1\text{H}$  NMR. The  $^1\text{H}$  NMR confirms the full deprotection of *tert*-butyl group. The methyl peak at 1.5 ppm was absent after deprotection and a slight shift of the methine peak from 3.25 to 3.45 ppm was observed (ESI, Figure S4, Supporting Information). More importantly, the removal of the *tert*-butyl group did not affect the integrity of polymer structures. The potential hydrolysis of ester bonds could not be detected.

Platinum–polymer conjugation has been intensively investigated using UV–vis in a previous study.<sup>23</sup> Briefly, CDDP was converted to its aquo form prior to conjugation to the polymer using the dicarboxylic acid group as ligand. The homopolymer was initially insoluble in aqueous solution. The necessary treatment with NaOH (2.5M) prior to the complexation to generate carboxylate ions gave highly water-soluble polymers. The subsequent conjugation of the polymer with *cis*-diamminediaqua platinum(II) complex was carried out at  $37^\circ\text{C}$  for 12 h. The

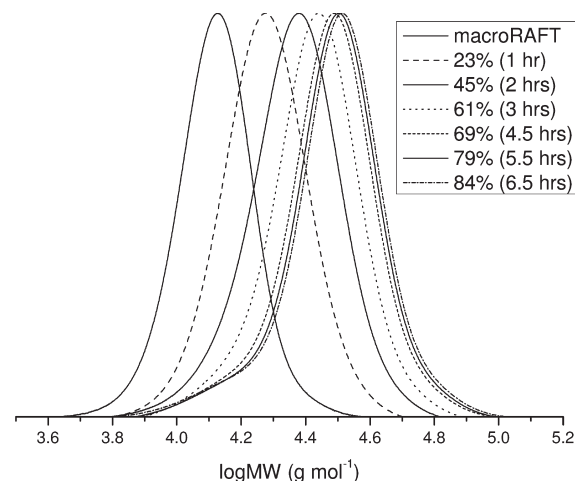
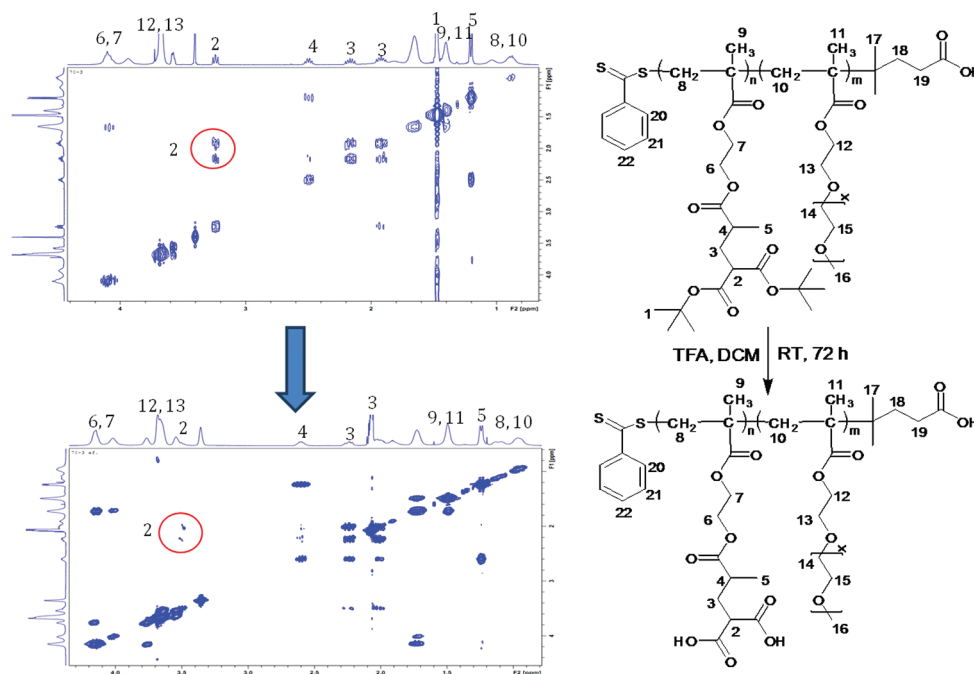


Figure 8. Molecular weight distribution obtained from SEC of the polymerization of PMAETC at  $70^\circ\text{C}$  in the presence of macro RAFT agent POEGMEMA<sub>50</sub> ( $[\text{MAETC}] = 0.5 \text{ mol L}^{-1}$ ,  $[\text{RAFT}] = 0.5 \times 10^{-2} \text{ mol L}^{-1}$ ,  $[\text{AIBN}] = 0.1 \times 10^{-2} \text{ mol L}^{-1}$  in Dioxane).

homopolymer showed a conjugation efficiency of around 60%. Complete conjugation was prevented by the occurring precipitation of the Pt-containing polymer in water (Figure 7). The increase in hydrophobicity is indicative for the attachment of platinum drugs. While the Pt–polymer conjugate appears to be insoluble in water or even NaOH solution, it shows good solubility in polar solvents such as DMF or DMAc. Therefore, cross-linking can be considered absent suggesting that the chelating ligand supports the formation of a stable six-membered ring (Figure 7). A list summarizing the solubilities of the polymer before and after conjugation can be found in Table S1, Supporting Information, ESI.

The investigation of the platinum–homopolymer conjugate highlighted the low water-solubility of PMAETC after platination in agreement with previous studies.<sup>23</sup> The hydrophobicity of this polymer inspired the subsequent formation of block copolymers with a water-soluble block in order to form micelles containing platinum drugs inside the core.

**Synthesis of Block Copolymers and Conjugation to Platinum Drugs.** RAFT polymerization<sup>40–44</sup> was demonstrated to be



**Figure 9.** COSY of diblockcopolymers before and after deprotection using trifluoroacetic acid (TFA) in dichloromethane at room temperature for 72 h.

a suitable method to prepare block copolymers, which can be subsequently assembled into micelles. There is only little concern in terms of toxicity of the RAFT end group.<sup>44–46</sup> In addition, the RAFT end group can be easily cleaved via aminolysis or other means allowing conjugation of a range of molecules.<sup>47</sup>

OEGMA has been chosen as the building block of the water-soluble shell due to its high biocompatibility. The high hydration of the PEG side chains prevents opsonin adsorption and the subsequent clearance and therefore results in long–long circulating carrier.<sup>48</sup>

In order to synthesize POEGMEMA-*block*-PMAETC, a macroRAFT agent (POEGMEMA) was first prepared by polymerization of OEGMEMA in acetonitrile at 70 °C with the presence of 4-cyanopentanoic acid dithiobenzoate (CPADB) as RAFT agent. The conversion of the monomer was determined via NMR spectroscopy by comparing the intensity of vinyl proton peak (6.1 and 5.6 ppm) to that of aliphatic proton peaks (1.1–1.3 ppm). An increase in the monomer conversion with reaction time according to pseudo first order kinetic and a narrow molecular weight distribution were observed (ESI-Figures S5–S7, Supporting Information). This finding is in agreements with literature.<sup>49,50</sup> The resulting polymer was purified by precipitation in anhydrous diethyl ether to remove all residual monomer, RAFT agent and AIBN.

POEGMEMA macroRAFT agent ( $M_{n,theo} = 15\,279\text{ g mol}^{-1}$ ,  $M_{n,SEC} = 11\,100\text{ g mol}^{-1}$ , PDI of 1.06) was employed in the subsequent polymerization of MAETC. The rate of polymerization was slightly faster than the homopolymerization while an inhibition period was absent (Figure 5). The SEC chromatograms in Figure 8 clearly depict the shift of the polymer peaks toward higher molecular weight. The measured molecular weight increased approximately linearly with conversion, although it deviated from the theoretical value due to the SEC calibration, and the PDI remained low ( $<1.2$ ) throughout the polymerization (Figure 6), indicating that the polymerization proceeded with good control.

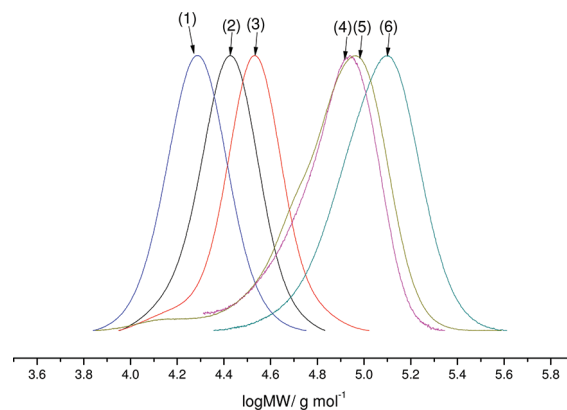


**Figure 10.** Molecular weight distribution obtained from SEC of block copolymers with variation of hydrophobic block length and their deprotection of di-*tert*-butyl groups: (1) BP-E27; (2) BP-E54; (3) BP-E80; (4) BP-E54 after deprotection; (5) BP-E27 after deprotection; (6) BP-E80 after deprotection.

Three POEGMEMA–PMAETC block copolymers, all with the same POEGMEMA block ( $M_{n,theo} = 15\,279\text{ g mol}^{-1}$ ,  $DP_n = 50$ ) but various PMAETC block lengths were deprotected and purified. The absence of the signals at 1.5 ppm (*tert*-butyl group) and a shift of the methine signal from 3.3 to 3.6 ppm were observed by COSY-NMR (Figure 9), which confirmed the successful deprotection. 2D NMR was deemed necessary since the methine signal was covered by the signal belonging to the PEG chain. After deprotection, a shift to higher molecular weight was observed (Figure 10), which is in opposition to the expected molecular weight loss and can only be explained by the altered hydrodynamic diameters. Table 1 summarizes the block copolymers used for further studies.

The three deprotected block copolymers from Table 1 (BP-E27, BP-E54, and BP-E80) were conjugated to platinum in a



**Table 1.** Molecular Weights and Number of Repeating Units of Polymers Used for Platination<sup>a</sup>

code	copolymers	$M_n^{\text{theo}}$ (g mol <sup>-1</sup> )	$M_n^{\text{GPC}}$ (g mol <sup>-1</sup> )	PDI	no. of RU, $N_{\text{OEGMEMA}}$	no. of RU, $N_{\text{MAETC}}$
BP-E27	POEGMEMA <sub>50</sub> - <i>b</i> -PMAETC <sub>27</sub>	26 457	18 100	1.09	50	27
BP-E54	POEGMEMA <sub>50</sub> - <i>b</i> -PMAETC <sub>54</sub>	37 635	24 100	1.10	50	54
BP-E80	POEGMEMA <sub>50</sub> - <i>b</i> -PMAETC <sub>80</sub>	48 399	29 800	1.12	50	80

<sup>a</sup>  $M_n^{\text{GPC}}$  determined by DMAc GPC using PSt calibration;  $M_n^{\text{NMR}}$  calculated by the following equation:  $M_n^{\text{NMR}} = [\text{I}^{\text{ppm}}/\text{I}^{\text{ppm}}] \times \text{MW}^{\text{MAETC}} + \text{MW}^{\text{MacroRAFT}}$ , where  $I^i$  are the integrals of peak at  $i$  ppm,  $\text{MW}^{\text{MAETC}}$  corresponds to molar mass of MAETC, and  $\text{MW}^{\text{MacroRAFT}}$  corresponds to molar mass of homopolymer of POEGMEMA.

**Table 2.** Loading Efficiency of Pt Drugs into Block Copolymers

polymeric platinum micelles	conjugation efficiency (%) <sup>c</sup>
BP-E27/Pt	82.9
BP-E54/Pt	75.0
BP-E80/Pt	64.9

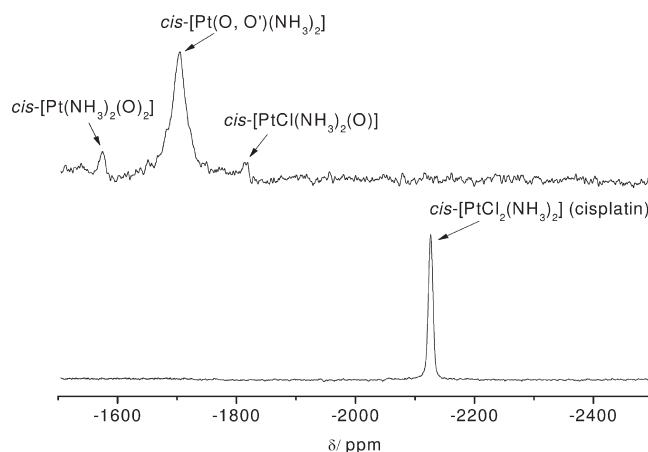
<sup>c</sup> The mol % of malonate with Pt attached.

procedure similar to that described above.<sup>23</sup> The platinum loading of the block copolymers was determined by TGA (ESI, Figure S8, Supporting Information) and ICP–MS. Table 2 summarizes the loading efficiencies for all block copolymers. While the loading efficiency of BP-E27 was around 83%, longer block length led to lower platinum loading. The Pt content in BP-E54 and BP-E80 decreased by 10% and even 20%, respectively. This is not surprising and is also in agreement with the low conjugation of the homopolymer. During the process, the carboxylic groups are deprotonated in the presence of NaOH creating fully water-soluble polymers. With the addition of platinum drugs, a hydrophobic polymer is formed causing in the case of the homopolymer precipitation and in the case of the block copolymer micelle formation. The polymers are dehydrated and further conjugation has been prevented.

An important analytical step is the investigation of the configuration of the attached complex. <sup>195</sup>Pt NMR can act here as a suitable tool to identify the different types of Pt complexes occurring (Figure 11). The signal at −2120 ppm of cisplatin shifted to lower field upon reaction with the polymer. The main species at −1710 ppm is indicative of the targeted structure although a small fraction with only one carboxylate ligand is in addition present. The shift is in agreement with literature values,<sup>51</sup> but even more important is that the measured low field shift in our earlier work<sup>23</sup> is indeed due to the involvement of other functional groups while here only the polymeric equivalent of carboplatin has been created.

Several factors were known to influence on the morphology of self-assembled aggregates including absolute and relative block length, the water content of the solvent mixture, the nature and the presence of additives such as ions, homopolymers, and surfactants, and the polydispersity of the block copolymer.<sup>52</sup> A focus of this work is the dependency of the block length of the hydrophobic block on the characteristics of the drug carrier.

The solubility of the PMAETC homopolymer is found to be pH dependent. In other words, it fully dissolves in aqueous solution at alkaline pH (~8–9), but the block is not soluble at neutral pH. Micelles from three POEGMEMA-*b*-PMAETC block copolymers of different hydrophobic block lengths (POEGMEMA<sub>50</sub>-*b*-PMAETC<sub>27</sub>, POEGMEMA<sub>50</sub>-*b*-PMAETC<sub>54</sub>,

**Figure 11.** <sup>195</sup>Pt NMR of copolymer conjugated to aquated *cis*-platinum drug and free platinum complex (CDDP). The Pt–polymer conjugate was dissolved in DI water and used D<sub>2</sub>O as a solvent to lock.

and POEGMEMA<sub>50</sub>-*b*-PMAETC<sub>80</sub>) were prepared by dissolving in DMF followed by dialysis against deionized water.

The size and shape of the aggregate was analyzed using DLS and TEM. DLS reveals an increase in micelle size with an increase of the PMAETC block length (Table 2), which was confirmed by TEM, although the sizes were slightly smaller (Figure 12). The difference in micelle size between DLS and TEM is attributed to the dehydrated state of the micelles. The increase in micelle size with increasing block length is in good agreement with the theory. With increasing ratio of the hydrophobic block the aggregation number increases to prevent entropically unfavorable excessive chain stretching.<sup>53</sup>

After Pt conjugation, the sizes increase significantly (Table 2) owing to the volume increase of the hydrophobic block. The presence of platinum is directly visible under the TEM. The heavy platinum signposts the location of the micelles clearly and no staining is required (Figure 12). The inset shows one micelle with a Janus-type structure.<sup>54</sup> Although a small ratio of these structures can be found throughout the sample, we are not confident enough to exclude that this is not only the result of the sample preparation only.

**Release of CDDP in Physiological Medium.** The release of the platinum drug from the polymer can be triggered by the presence of chloride ions, which will lead to ligand exchange of the platinum complex from carboxylate ligand to chloride ligand. The drug is then cleaved from the polymer as *cis*-diamminedichloroplatinum(II) (CDDP), which is the commercially available and FDA approved drug cisplatin. This process is favored in the presence of high amounts of chlorides, but not in chloride free buffers. Buffers such as the chloride containing phosphate buffered saline (PBS) or simple saline (0.9%) can force the release of CDDP.

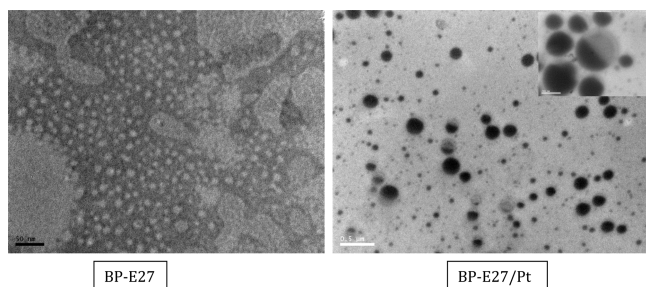


**Figure 12.** Transmission electron microscopy (TEM) of block copolymer before platination (BP-E27) and block copolymer after platination (BP-E27/Pt). Scale bar is 50 nm (left), 500 nm (right), and 200 nm for the small image.

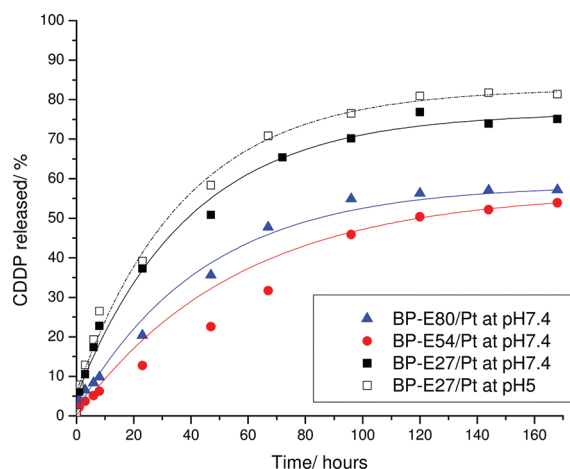


**Figure 13.** Release of CDDP from polymeric micelles in buffer saline solution (0.9%). The straight lines were fitted according to % CDDP Release =  $A \exp(-t/(\tau)) + y_0$ .

The macromolecular platinum complex reveals a high stability in distilled water and only insignificant fractions of platinum complex have been released over a prolonged period of time. However, in a physiological medium with 0.9% of sodium chloride the release of CDDP is immediately initiated. ICP-MS was used to investigate the amount of CDDP released. This method has been applied in previous studies<sup>23</sup> and is among the most common instrumental methods used for the analysis of trace elements including platinum.

The release of the CDDP from micellar solutions containing BP-E27/Pt, BP-E54/Pt, and BP-E80/Pt has been monitored over 1 week (Figure 13). No initial burst of the drug was observed in all polymeric platinum conjugates and the release appears to reach a plateau at around 50–70%. Similar results were also observed in our previous study, only that the release plateaued already at 40% of drug released.<sup>23</sup> The incomplete release of all conjugated CDDP can be attributed to the resulting polymer structure after release, which contains a high content of negative charges due to the presence of carboxylic groups. In other words, further release of CDDP yields an unfavorable increase in charge density. In addition, the maximum amount of drug released here is noticeable higher to the previous data (40%), where the structure of the complex probably involved a sulfur ligand.<sup>23</sup> The better release in this work could then be due to the absence of stronger bond of Pt–S, but it also needs to be considered that the block sizes are different and therefore direct comparison is difficult. Interestingly, the release of platinum drug

**Table 3.** Hydrodynamic Diameter Obtained via DLS before and after Pt Conjugation

code	micelles	hydrodynamic diameter/nm	
		before conjugation in water	after conjugation in water
BP-E27	POEGMEMA <sub>50</sub> - <i>b</i> -PMAETC <sub>27</sub>	31.92 ± 1.32	76.67 ± 0.30
BP-E54	POEGMEMA <sub>50</sub> - <i>b</i> -PMAETC <sub>54</sub>	42.53 ± 1.69	98.19 ± 1.35
BP-E80	POEGMEMA <sub>50</sub> - <i>b</i> -PMAETC <sub>80</sub>	52.79 ± 1.20	175.77 ± 3.78

**Table 4.** Hydrodynamic Diameter of Micelles, Measured by DLS in Water, before and after Platinum Release

code	micelles	hydrodynamic diameter/nm	
		before Pt released	after Pt released
BP-E27	POEGMEMA <sub>50</sub> - <i>b</i> -PMAETC <sub>27</sub>	76.67 ± 0.30	6.39 ± 0.88
BP-E54	POEGMEMA <sub>50</sub> - <i>b</i> -PMAETC <sub>54</sub>	98.19 ± 1.35	5.97 ± 0.70
BP-E80	POEGMEMA <sub>50</sub> - <i>b</i> -PMAETC <sub>80</sub>	175.77 ± 3.78	6.38 ± 0.19

was accompanied by the formation of carboxylate groups, which increases the water solubility of the block copolymers. This eventually led to fully soluble polymers as proven by DLS measurement of the hydrodynamic diameter ( $\sim 6$  nm) after 1 week (Table 3).

Another noteworthy result was a considerable difference in release rate (Table 4) from the micelles prepared from block copolymers with varying hydrophobic length. The shorter hydrophobic length was found to lead to a faster release. Around 70% of conjugated platinum drug was released from BP-E27/Pt after 3 days, while the rate of release is noticeably slower from micelles with bigger hydrophobic cores (Figure 13). The faster rate of release can be assigned to the lower stability of the micelle. After a shorter period of time enough CDDP has been released to significantly increase hydrophilicity of the core allowing faster penetration of saline solution.

Although investigation at blood pH value is important, it needs to be considered that micelles will go through a cascade of different localization traveling from the cell exterior to the cytosol. Upon uptake via endocytosis, the micelle is located in the slightly acidic endosomes (pH 5.0–5.5) and lysosomes (pH 4.0–4.5).<sup>56–58</sup> Therefore, the release of polymeric platinum micelles (BP-E27/Pt) was investigated in pH7.4 and pH5 sodium chloride solution. Initially, the effects of pH on the release properties can be neglected during the first 48 h. After a few days, a slight increase of the amount of released CDDP can be observed, which can be attributed to higher protonation degree and thus, lower charge density.

For a more quantitative assessment of the data, the curves in Figure 13 were fitted with a simple model assuming first-order kinetics:

$$\% \text{ CDDP Release} = A \exp\left(-\frac{t}{\tau}\right) + y_0 \quad (1)$$

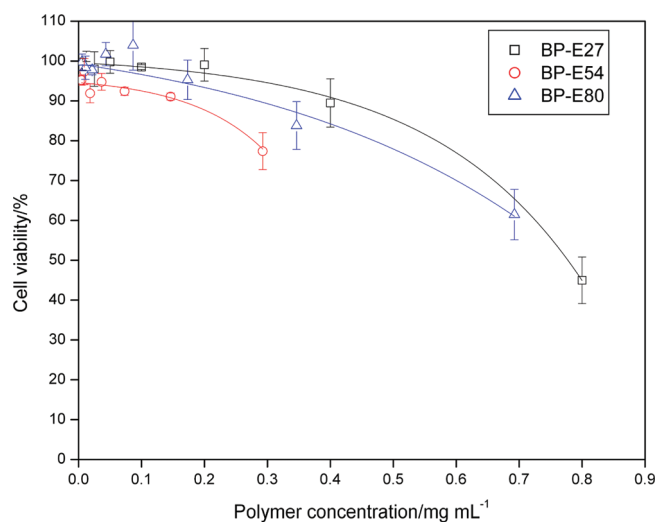
( $t$  is time in hours,  $\tau$  is the release constant)

The release constant  $\tau$  of all systems as summarized in Table 5. The fitted curves were included in Figure 13.

**Table 5.** Determination of Released Constant  $\tau$  by Fitting Equation 1 To Release Data Displayed in Figure 13 Compared with IC<sub>50</sub> Values of the Polymer Only and the Pt-Conjugated Polymer

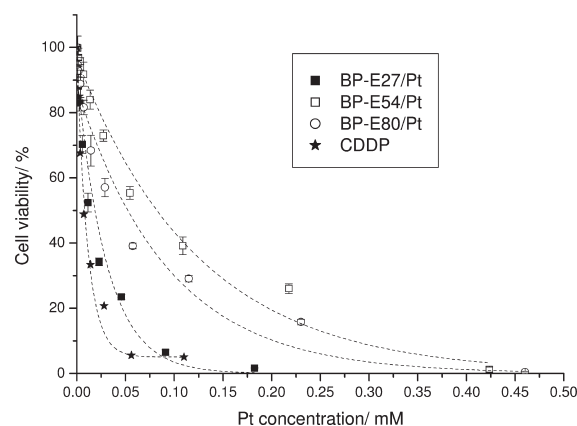
samples	$\tau$ (h)	$R^2$	IC <sub>50</sub> (polymer) ( $\mu\text{g mL}^{-1}$ )	IC <sub>50</sub> (Pt–polymer) c[Pt] ( $\mu\text{M}$ )	IC <sub>50</sub> (Pt–polymer) c[polymer] ( $\mu\text{g mL}^{-1}$ )
BP-E27 at pH 5	37.5	0.990	-	-	-
BP-E27 at pH 7.4	39.2	0.989	730	19.7	23.5
BP-E54 at pH 7.4	56.27	0.946	<sup>a</sup>	82.3	76.5
BP-E80 at pH 7.4	44.13	0.989	<sup>a</sup>	54.1	50.2
CDDP	-	-	-	7.2	-
carboplatin from ref 55	-	-	-	27	-

<sup>a</sup> Cannot be determined from Figure 14, but IC<sub>50</sub> values are estimated to be within similar range to BP-E27.

**Figure 14.** Percentage of living A 549 cell after being exposed to block copolymer micelle solutions including BP-E27, BP-E54, and BP-E80 for 72 h.

**Cytotoxicity of Polymers.** The biocompatibility of copolymers including BP-E27, BP-E54, and BP-E80 was tested prior to platinum conjugation on a human lung cancer cell line (A549). All samples were sterilized under UV light for 30 min before incubating with the cancer cell lines. The sulforhodamine B (SRB) assay was employed to determine the cytotoxicity of the polymers after an incubation time of 72 h. Different concentrations of the polymers ranging from 0 to 0.8  $\text{mg mL}^{-1}$  were exposed to A549. The IC<sub>50</sub> values (the concentration at which there is 50% growth inhibition relative to control), are around 0.7  $\text{mg mL}^{-1}$ , which is well above the concentration typically used for drug delivery systems (Figure 14). This is in agreement with many previous studies, in which the RAFT end group (CPADB) is only of little concern in regards to cytotoxicity.<sup>45,46,59–62</sup>

Polymeric platinum micelles obtained by conjugation of platinum drugs to BP-E27, BP-E54, or BP-E80 were used to assess the anti-cancer activity. The cell viability was recorded against the platinum concentration in each micelle solution (Figure 15). Micelles based on BP-E27/Pt were the most active in suppressing cancer cell growth among the tested micelles. This can be explained by the fast platinum release during the first 72 h according to Figure 13. The IC<sub>50</sub> values were determined using the logarithmic concentration<sup>63</sup> of the polymer before and after platinum conjugation. To be able to compare these data with cisplatin and carboplatin, the amount of Pt in each polymer were calculated (Supporting Information, Table S2). None of the polymeric platinum micelles was found to be more

**Figure 15.** Living cell percentage after being exposed to free platinum drug and platinum polymeric micelles, namely BP-E27/Pt, BP-E54/Pt, and BP-E80/Pt, for 72 h.

effective than CDDP itself, but BP-E27/Pt is more effect than carboplatin, which is the parent drug of this macromolecular system (Table 5). There are several reasons for the lower toxicity compared to cisplatin. The most obvious is that after 72 h, the release of CDDP from the micelles is not yet complete. Although prior experiments cannot exactly mimic the environment in the cell, platinum release results showed that only a maximum of 50–70% of platinum release can be achieved. Therefore, the actual amount of available platinum was much lower than the initial platinum concentration. The drug release experiments can indeed act as an indication for the toxicity of the drug carrier. Listed in Table 5 are the IC<sub>50</sub> values side by side with  $t$ , the release parameter. Indeed, the fastest release coincides with the highest toxicity while the slowest rate of cisplatin release led to the highest IC<sub>50</sub> values. In addition, the cell line chosen, A549, is highly responsive to the treatment with CDDP. Nanoparticles would be expected to have more effect in platinum resistant cell lines where they can help bypassing resistance mechanisms.

More detailed in vitro evaluations are currently being undertaken to investigate the biological effects of these polymeric micelles.

## CONCLUSION

A novel monomer with a neighboring carboxylate functional group was synthesized via Michael addition. Subsequently, RAFT polymerization was employed to generate different block copolymers composed of POEGMEMA and the synthesized monomer, MAETC. The polymerization was well controlled and a range of block copolymers were obtained. The block length was



found to play an important role in the preparation of the drug carrier. While a shorter PMAETC block led to higher Pt–drug loading, it also enabled better and faster drug release. In addition, the micelles were typically smaller. This combination led to a more toxic carrier when testing the cell viability of A549 lung cancer cells. These initial biological evaluations should only indicate the feasibility of this approach. More detailed investigations are underway to understand better the cellular uptake of these micelles in dependency of the micelle stability.

## ■ ASSOCIATED CONTENT

**S Supporting Information.**  $^{13}\text{C}$ , DEPT-135, DEPT-90 NMR spectrum of purified monomer, molecular weight distribution obtained from SEC of the polymerization of PMAETC,  $^1\text{H}$  NMR spectrum of purified homopolymer PMAETC,  $^1\text{H}$  NMR of PMAETC homopolymer before and after deprotection, kinetic plots of the polymerization of POEGMEMA, TGA analysis of CDDP and block copolymer conjugated to platinum, and solubility of PMAETC homopolymer and PMAETC conjugated to CDDP. This material is available free of charge via the Internet at <http://pubs.acs.org/>.

## ■ AUTHOR INFORMATION

### Corresponding Author

\*E-mail: m.stenzel@unsw.edu.au.

## ■ ACKNOWLEDGMENT

M.H.S. thanks the ARC (Australian Research Council) for funding in form of a Future Fellowship (FT0991273) and a Discovery Project (DP1092694). V.T.H. thanks the Australian government for Endeavour Postgraduate Award. P.D.S. thanks the Prostate Cancer Foundation of Australia for a project grant (# PG3009). The authors would like to thank the Centre for Advanced Macromolecular Design (CAMD) and UNSW Analytical Centre for support. We would also like to thank Dr Ying Song from MIT for initiating a valuable discussion on  $^{195}\text{Pt}$  NMR

## ■ REFERENCES

- Reedijk, J. *Proc. Natl. Acad. Sci. U.S.A.* **2003**, *100* (7), 3611–3616.
- Kelland, L. *Nat. Rev. Cancer* **2007**, *7* (8), 573–584.
- Boulikas, T.; Vougiouka, M. *Oncol. Rep.* **2003**, *10* (6), 1663–1682.
- Rosenberg, B. *Interdisciplinary Sci. Rev.* **1978**, *3* (2), 134–147.
- Lippert, B. *Coord. Chem. Rev.* **1999**, *182*, 263–295.
- Hambley, T. W. *Coord. Chem. Rev.* **1997**, *166*, 181–223.
- Galanski, M.; Jakupiec, M. A.; Keppler, B. K. *Curr. Med. Chem.* **2005**, *12* (18), 2075–2094.
- Ho, Y. P.; Au-Yeung, S. C. F.; To, K. K. W. *Med. Res. Rev.* **2003**, *23* (5), 633–655.
- Zutphen, S. v.; Reedijk, J. *Coord. Chem. Rev.* **2005**, *249* (24), 2845–2853.
- Wang, K.; Lu, J. F.; Li, R. C. *Coord. Chem. Rev.* **1996**, *151*, 53–88.
- Yu, F.; Megyesi, J.; Price, P. M. *Am. J. Physiol.-Renal Physiol.* **2008**, *295* (1), F44–F52.
- Stenzel, M. H. *Chem. Commun. (Cambridge, U. K.)* **2008**, *30*, 3486–3503.
- Uhrich, K. E.; Cannizzaro, S. M.; Langer, R. S.; Shakesheff, K. M. *Chem. Rev.* **1999**, *99* (11), 3181–98.
- Allen, C.; Maysinger, D.; Eisenberg, A. *Colloid Surf. B: Biointerfaces* **1999**, *16* (1–4), 3–27.
- Haxton, K. J.; Burt, H. M. *J. Pharm. Sci.* **2009**, *98* (7), 2299–2316.
- Komane, L.; Mukaya, E.; Neuse, E.; van Rensburg, C. *J. Inorg. Organomet. Polym. Mater.* **2008**, *18* (1), 111–123.
- Nishiyama, N.; Kataoka, K. *J. Controlled Release* **2001**, *74* (1–3), 83–94.
- Mizumura, Y.; Matsumura, Y.; Hamaguchi, T.; Nishiyama, N.; Kataoka, K.; Kawaguchi, T.; Hrushesky, W. J. M.; Moriyasu, F.; Kakizoe, T. *Jpn. J. Cancer Res.* **2001**, *92* (3), 328–336.
- Nishiyama, N.; Okazaki, S.; Cabral, H.; Miyamoto, M.; Kato, Y.; Sugiyama, Y.; Nishio, K.; Matsumura, Y.; Kataoka, K. *Cancer Res.* **2003**, *63* (24), 8977–8983.
- Bontha, S.; Kabanov, A. V.; Bronich, T. K. *J. Controlled Release* **2006**, *114* (2), 163–174.
- Knox, R. J.; Friedlos, F.; Lydall, D. A.; Roberts, J. J. *Cancer Res.* **1986**, *46* (4 Part 2), 1972–1979.
- Sood, P.; Thurmond, K. B.; Jacob, J. E.; Waller, L. K.; Silva, G. O.; Stewart, D. R.; Nowotnik, D. P. *Bioconjugate Chem.* **2006**, *17* (5), 1270–1279.
- Huynh, V. T.; Chen, G.; Souza, P. d.; Stenzel, M. H. *Biomacromolecules* **2011**, *12* (5), 1738–1751.
- Bergman, E. D.; Ginsburg, D.; Pappo, R. *Organic React.* **1959**, *10*, 179–556.
- Johnson, M. T.; Komane, L. L.; N'Da, D. D.; Neuse, E. W. *J. Appl. Polym. Sci.* **2005**, *96* (1), 10–19.
- Geng, Y.; Dalhaimer, P.; Cai, S.; Tsai, R.; Tewari, M.; Minko, T.; Discher, D. E. *Nat. Nano* **2007**, *2* (4), 249–255.
- Mitsukami, Y.; Donovan, M. S.; Lowe, A. B.; McCormick, C. L. *Macromolecules* **2001**, *34* (7), 2248–2256.
- Oae, S.; Okabe, T.; Yagihara, T. *Tetrahedron* **1972**, *28* (12), 3203–8.
- Ye, H.; Jin, L.; Hu, R.; Yi, Z.; Li, J.; Wu, Y.; Xi, X.; Wu, Z. *Biomaterials* **2006**, *27* (35), 5958–5965.
- Haxton, K. J.; Burt, H. M. *Dalton Trans.* **2008**, *43*, 5872–5875.
- Skehan, P.; Storeng, R.; Scudiero, D.; Monks, A.; McMahon, J.; Vistica, D.; Warren, J. T.; Bokesch, H.; Kenney, S.; Boyd, M. R. *J. Natl. Cancer Inst.* **1990**, *82* (13), 1107–1112.
- Mather, B. D.; Viswanathan, K.; Miller, K. M.; Long, T. E. *Prog. Polym. Sci.* **2006**, *31* (5), 487–531.
- Clemens, R. J.; Rector, F. D. *J. Coat. Technol. Res.* **1989**, *61*, 83–91.
- Cregge, R. J.; Herrmann, J. L.; Richman, J. E.; Romanet, R. F.; Schlessi, Rh. *Tetrahedron Lett.* **1973**, *28*, 2595–2598.
- Herrmann, J. L.; Richman, J. E.; Schlessi, Rh. *Tetrahedron Lett.* **1973**, *28*, 2599–2602.
- Wang, M.-X.; Miao, W.-S.; Cheng, Y.; Huang, Z.-T. *Tetrahedron* **1999**, *55* (51), 14611–14622.
- Valentine, J. S.; Curtis, A. B. *J. Am. Chem. Soc.* **1975**, *97* (1), 224–226.
- Christensen, J. J.; Hill, J. O.; Izatt, R. M. *Science* **1971**, *174* (4008), 459–467.
- Perrier, S.; Barner-Kowollik, C.; Quinn, J. F.; Vana, P.; Davis, T. P. *Macromolecules* **2002**, *35* (22), 8300–8306.
- Moad, G.; Thang, S. H. *Aust. J. Chem.* **2009**, *62* (11), 1379–1381.
- Moad, G.; Rizzardo, E.; Thang, S. H. *Aust. J. Chem.* **2009**, *62* (11), 1402–1472.
- Moad, G.; Rizzardo, E.; Thang, S. H. *Aust. J. Chem.* **2005**, *58* (6), 379–410.
- Moad, G.; Chong, Y. K.; Postma, A.; Rizzardo, E.; Thang, S. H. *Polymer* **2005**, *46* (19), 8458–8468.
- Gregory, A.; Stenzel, M. H. *Expert Opin. Drug Deliv.* **2011**, *8* (2), 237–269.
- Stenzel, M. H.; Barner-Kowollik, C.; Davis, T. P.; Dalton, H. M. *Macromol. Biosci.* **2004**, *4* (4), 445–453.
- Chang, C. W.; Bays, E.; Tao, L.; Alconcel, S. N. S.; Maynard, H. D. *Chem. Commun. (Cambridge, U. K.)* **2009**, *24*, 3580–3582.
- Alconcel, S. N. S.; Grover, G. N.; Matsumoto, N. M.; Maynard, H. D. *Aust. J. Chem.* **2009**, *62* (11), 1496–1500.
- Stolnik, S.; Illum, L.; Davis, S. S. *Adv. Drug Delivery Rev.* **1995**, *16* (2–3), 195–214.

- (49) Mertoglu, M.; Garnier, S.; Laschewsky, A.; Skrabania, K.; Storsberg, J. *Polymer* **2005**, *46* (18), 7726–7740.
- (50) Becer, C. R.; Hahn, S.; Fijten, M. W. M.; Thijs, H. M. L.; Hoogenboom, R.; Schubert, U. S. *J. Polym. Sci., Part A: Polym. Chem.* **2008**, *46* (21), 7138–7147.
- (51) Berners-Price, S. J.; Ronconi, L.; Sadler, P. J. *Prog. Nucl. Magn. Reson. Spectrosc.* **2006**, *49* (1), 65–98.
- (52) Lim Soo, P.; Eisenberg, A. *J. Polym. Sci., Part B: Polym. Phys.* **2004**, *42* (6), 923–938.
- (53) Cameron, N. S.; Corbierre, M. K.; Eisenberg, A. *Can. J. Chem.* **1999**, *77* (8), 1311–1326.
- (54) Christian, D. A.; Tian, A. W.; Ellenbroek, W. G.; Levental, I.; Rajagopal, K.; Janmey, P. A.; Liu, A. J.; Baumgart, T.; Discher, D. E. *Nat. Mater.* **2009**, *8* (10), 843–849.
- (55) Edelman, M.; Quam, H.; Mullins, B. *Cancer Chemother. Pharmacol.* **2001**, *48* (2), 141–144.
- (56) Park, H. S.; Kim, C.; Lee, H. J.; Choi, J. H.; Lee, S. G.; Yun, Y. P.; Kwon, I. C.; Lee, S. J.; Jeong, S. Y.; Lee, S. C. *Nanotechnology* **2010**, *21* (22), No. in press.
- (57) Yang, Q.; Wang, S.; Fan, P.; Wang, L.; Di, Y.; Lin, K.; Xiao, F.-S. *Chem. Mater.* **2005**, *17* (24), 5999–6003.
- (58) Lee, H. J.; Kim, S. E.; Kwon, I. K.; Park, C.; Kim, C.; Yang, J.; Lee, S. C. *Chem. Commun.* **2010**, *46* (3), 377–379.
- (59) Nguyen, T. L. U.; Farrugia, B.; Davis, T. P.; Barner-Kowollik, C.; Stenzel, M. H. *J. Polym. Sci., Part A: Polym. Chem.* **2007**, *45* (15), 3256–3272.
- (60) Pissuwan, D.; Boyer, C.; Gunasekaran, K.; Davis, T. P.; Bulmus, V. *Biomacromolecules* **2010**, *11* (2), 412–420.
- (61) Beattie, D.; Wong, K. H.; Williams, C.; Poole-Warren, L. A.; Davis, T. P.; Barner-Kowollik, C.; Stenzel, M. H. *Biomacromolecules* **2006**, *7* (4), 1072–1082.
- (62) Duong, H. T. T.; Nguyen, T. L. U.; Kumpfmüller, J.; Stenzel, M. H. *Aust. J. Chem.* **2010**, *63* (8), 1210–1218.
- (63) Cai, S.; Vijayan, K.; Cheng, D.; Lima, E.; Discher, D. *Pharm. Res.* **2007**, *24* (11), 2099–2109.